Design of all-solid leakage channel fibers with large mode area and low bending loss

Kunimasa Saitoh[1*], Yukihiro Tsuchida[1], Lorenzo Rosa[1], Masanori Koshiba[1], Federica Poli[2], Annamaria Cucinotta[2], Stefano Selleri[2], Mrinmay Pal[3], Mukul Paul[3], Debashri Ghosh[3], and Shyamal Bhadra[3]

[1]Graduate School of Information Science and Technology, Hokkaido University, Sapporo 060-0814, Japan
[2]Information Engineering Department, University of Parma, I-43100 Parma, Italy
[3]Fibre Optics Division, Central Glass & Ceramic Research Institute, Kolkata - 700032, India
[*]ksaitoh@ist.hokudai.ac.jp

Abstract: We investigate a novel design for all-solid large mode area (LMA) leakage channel fibers (LCFs) for high-power Yb-doped fiber lasers and amplifiers, based on a single down-doped-silica rod ring surrounding a seven-cell pure-silica core, aiming for effectively single-mode behavior and low bending loss characteristics. Through detailed numerical simulations based on the finite element method (FEM), we find that the proposed all-solid LMA-LCFs, having a seven-cell core and two different sizes of down-doped rods, can achieve sufficient differential mode loss and much lower bending loss, as compared with a previously-reported LCF with a one-cell core and six large down-doped-silica rods.

References and links

1. Y. Jeong, J.K. Sahu, D.N. Payne, and J. Nilsson, "Ytterbium-doped large-core fibre laser with 1 kW of continuous-wave output power," Electron. Lett. **40**, 470-472 (2004).
2. P. Wang, L. J. Cooper, J. K. Sahu, and W. A. Clarkson, "Efficient single-mode operation of a cladding-pumped ytterbium-doped helical-core fiber laser," Opt. Lett. **31**, 226–228 (2006).
3. J.M. Fini, "Design of large-mode-area amplifier fibers resistant to bend-induced distortion," J. Opt. Soc. Am. B **24**, 1669-1676 (2007).
4. A. Galvanauskas, "Mode-scalable fiber-based chirped pulse amplification systems," IEEE J. Sel. Top. Quantum Electron. **7**, 504-517 (2001).
5. M.D. Nielsen, J.R. Folkenberg, and N.A. Mortensen, "Singlemode photonic crystal fibre with effective area of 600 μm^2 and low bending loss," Electron. Lett. **39**, 1802-1803 (2003).
6. W.S. Wong, X. Peng, J.M. McLanghlin, and L. Dong, "Breaking the limit of maximum effective area for robust single-mode propagation in optical fibers," Opt. Lett. **30**, 2855-2857 (2005).
7. L. Dong, J. Li, and X. Peng, "Bend-resistant fundamental mode operation in ytterbium-doped leakage channel fibers with effective areas up to 3160 μm^2," Opt. Express **14**, 11512-11519 (2006).
8. X. Peng and L. Dong, "Fundamental-mode operation in polarization-maintaining ytterbium-doped fiber with an effective area of 1400 μm^2," Opt. Lett. **32**, 358-360 (2007).
9. L. Dong, X. Peng, and J. Li, "Leakage channel optical fibers with large effective area," J. Opt. Soc. Am. B **24**, 1689-1697 (2007).
10. L. Dong, J. Li, H. McKay, A. Marcinkevicius, B. Thomas, M. Moore, L. Fu, and M.E. Fermann, "Robust and practical optical fibers for single mode operation with core diameters up to 170 μm." presented at Conference on Lasers and Electro-Optics and Quantum Electronics and Laser Science Conference 2008 (CLEO/QELS 2008), San Jose, Calif., May 2008.
11. L. Dong, T.W. Wu, H.A. McKay, L. Fu, J. Li, and H.G. Winful, "All-glass large-core leakage channel fibers," IEEE J. Sel. Topics Quantum Electron. **15**, 47-53 (2009).
12. K. Saitoh and M. Koshiba, "Full-vectorial imaginary-distance beam propagation method based on a finite element scheme: application to photonic crystal fibers," IEEE J. Quantum Electron. **38**, 927-933 (2002).
13. K. Kakihara, N. Kono, K. Saitoh, and M. Koshiba, "Full-vectorial finite element method in a cylindrical coordinate system for loss analysis of photonic wire bends," Opt. Express **14**, 11128-11141 (2006).
14. Y. Tsuchida, K. Saitoh, and M. Koshiba, "Design of single-moded holey fibers with large-mode-area and low bending losses: The significance of the ring-core region," Opt. Express **15**, 1794-1803 (2007).

1. Introduction

The development of innovative technologies for high-power fiber lasers and amplifier is driven by a persistent industrial demand for their enhancement in a wide spectrum of applications and power ranges, from tens of watts to many kilowatts [1-3]. In this context, the technical progress in the field of large-mode-area (LMA) single-mode optical fibers permits an effective solution to the main problem in the development of high-power Yb^{3+}-doped fiber lasers, that is the suppression of nonlinear effects, such as self-phase modulation, Raman scattering, and Brillouin scattering, in both continuous wave and mode-locked fiber lasers. This can be controlled through the employment of LMA optical fibers, when the numerical aperture (NA) is reduced to suppress the multi-mode behavior typical of such large-core fibers, at the price of a significant increase of the macro-bending loss. This can be addressed through the deployment of specially-designed optical fibers with higher NA that can achieve an effectively single-mode operation regime by limiting the propagation of the higher-order modes. However, while in the standard fibers the core diameter cannot be raised over 30 μm due to the onset of multi-mode behaviors [4], if we consider the all-silica photonic crystal fibers (PCFs), which would permit to obtain very broad-band single-mode LMA operation, a very similar diameter limit is encountered due to the increase of the bending losses [5].

These issues common to LMA single-mode fibers have recently been addressed by the introduction by Dong *et al.* of the leakage channel fibers (LCFs) [6-9], characterized by a cladding formed by a single air-hole ring. While these fibers are inherently lossy, as they only support leaky guided modes, the precise tuning of the air-hole pitch and diameters offers enough degrees of freedom to independently engineer the confinement loss (CL) of the different modes. In particular, it is possible to selectively achieve a high confinement loss (CL) for all the higher-order modes (HOMs), while the fundamental mode (FM) CL can be kept low enough to allow almost unhindered propagation. However, LCFs with an array of air-holes around the core require to be sealed and the resulting refractive index perturbations can lead to mode distortion, having an even larger impact on the mode structure due to the large core size [10, 11]. Therefore, to reduce mode distortion and achieve an easier LCF fabrication, an all-glass LCF design has recently been proposed [10, 11], in which the air-holes are replaced by fluorine-doped silica rods, whose refractive index is lower than that of pure silica. The reported all-glass LCF design is characterized by a one-cell pure-silica core surrounded by six large down-doped silica rods, and while its LP_{11}-like HOM CL, CL_{2nd}, is larger than 1 dB/m and the FM CL, CL_{fund}, is lower than 0.1 dB/m, its bending loss is not low enough for the intended applications [11].

In this paper, we propose and numerically investigate a novel design for single-mode all-glass LCFs having LMA and low bending loss, in which the microstructured optical fiber is formed by a single fluorine-doped silica-glass rod ring, while the solid core region is built by introducing multiple pure-silica rods. For the simulations, we have employed a full-vector FEM (V-FEM) [12, 13] solver using perfectly matched layers. Through a detailed modal analysis based on V-FEM, we evaluated the effective area, A_{eff}, and the loss variations as a function of the rod spacing, or pitch, Λ and the normalized rod diameter d/Λ. It is thus shown that the proposed all-solid LMA-LCFs with a seven-cell core and two different sizes of down-doped rods achieve sufficient differential mode loss and lower bending loss, when compared to the aforesaid LCF with a one-cell core and six large down-doped-silica rods, at the 1064-nm operating wavelength of interest for high-power Yb-doped fiber lasers and amplifiers.

2. All-glass leakage channel fiber design and numerical results

Figure 1 shows the cross-sections of the considered all-glass LCFs. Figure 1(a) depicts the all-glass LCF formed by six fluorine-doped silica rods, whose solid core is created by introducing one pure-silica rod (this design will be denoted from now on as LCF1). The fluorine-doped silica rod diameter is *d* and the center-to-center rod spacing is Λ. Figure 1(b) details the all-glass LCF formed by twelve fluorine-doped silica rods, where now the solid core is created by

introducing seven pure-silica rods (LCF7). The background material is also pure silica and the relative refractive index difference between the two kinds of material is defined as

$$\Delta^- = \frac{n^2 - n_F^2}{2n^2} \times 100 \quad [\%],$$

where n is the index of pure silica and n_F is the index of fluorine-doped silica. In the following calculations, we will assume $\Delta^- = 0.1\%$ for all the LCF designs, namely the refractive index of fluorine-doped silica is 0.00145 below that of pure silica. Notice that a small variation of Δ^- does not affect the bending loss characteristics of the all-glass LCFs.

Differently from the standard step-index fiber, all modes in the LCFs are inherently leaky because the core refractive index is the same as the outer cladding region one. However, by tuning Λ and d it is possible to have enough degrees of freedom to independently engineer the CL of the different modes, which cannot be obtained in conventional optical fibers. In this way, while keeping the FM CL $CL_{fund} < 0.1$ dB/m, the HOM CL can be increased so that $CL_{2nd} > 1$ dB/m, thus obtaining an effectively single-mode behavior. In addition, the target effective area is set to $A_{eff} = 1400$ μm^2 (i.e. a core diameter around 50 μm) at 1064 nm for the purpose of avoiding unwanted nonlinear effects.
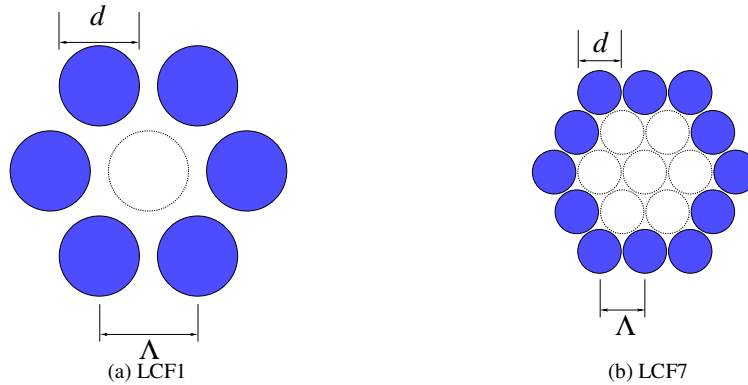
Fig. 1. Schematic cross-section of all-glass leakage channel fibers formed by (a) 6 fluorine-doped silica rods surrounding a one-cell silica core (LCF1) and (b) 12 fluorine-doped silica rods surrounding a seven-cell silica core (LCF7).
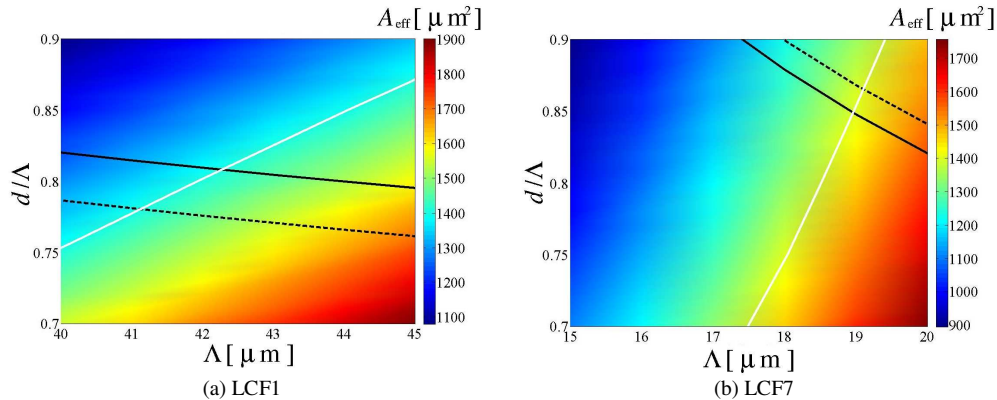
Fig. 2. Effective area of FM at 1064 nm as a function of the design parameters Λ and d/Λ for (a) LCF1 and (b) LCF7. The curves denote conditions on $A_{eff} = 1400$ μm^2 (white), $CL_{2nd} = 1$ dB/m (solid black), and $CL_{fund} = 0.1$ dB/m (dashed black).
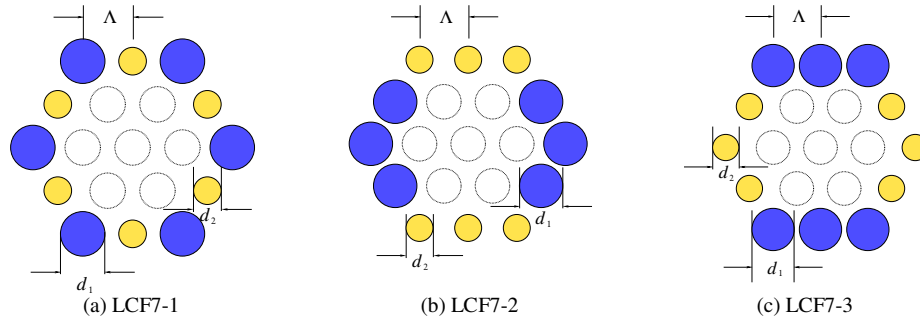
Fig. 3. Schematic depiction of the modified types of LCF7, having fluorine-doped silica rods of two different diameters d_1 and d_2.

Figures 2(a) and 2(b) show the contour plots of the effective area (color maps) of the degenerated HE_{11} FM at 1064 nm, mapped as a function of the design parameters Λ and d/Λ, for LCF1 and LCF7, respectively. The refractive index of silica is assumed to be $n = 1.45$, with $\Delta^- = 0.1\%$. In order to simply visualize the condition on the target value $A_{\mathrm{eff}} = 1400$ μm^2, we depict it with a solid white curve in Fig. 2. The solid black curve in the same graphs corresponds to a CL value of 1 dB/m at 1064 nm for the HOM, namely, the LP_{11}-like group formed by the TE_{01} mode, the TM_{01} mode, and the degenerated HE_{21} mode. This value is enough to guarantee the suppression of HOM propagation in high-power Yb-doped fiber lasers and amplifiers in practical applications [9]. In addition, we assume that the maximum FM CL limit is 0.1 dB/m, in order to ensure negligible transmission loss. The dashed black curve, shown in Fig. 2, corresponds to a FM CL of 0.1 dB/m at 1064 nm. From these results, we can clearly observe that for the LCF1 the solid curve lies above the dashed one. This means that the LCF1 offers the chance of simultaneously fulfilling both constraints, because the CL of all modes decreases as the value of d/Λ increases. Moreover, we can determine the values of the structural parameters Λ and d/Λ that permit effectively single-mode operation ($CL_{\mathrm{fund}} < 0.1$ dB/m and $CL_{\mathrm{2nd}} = 1$ dB/m) at the target effective area, resulting in $\Lambda = 42.3$ μm and $d/\Lambda = 0.81$ in the LCF1 case. On the contrary, the LCF7 has no possibility to simultaneously fulfill both constraints, because of the opposite relationship between the FM and HOM CL shown in Fig. 2(b).

In order to achieve the effectively single-mode condition as defined by $CL_{\mathrm{fund}} < 0.1$ dB/m and $CL_{\mathrm{2nd}} > 1$ dB/m in the all-solid LCF7 structure, we considered a modified version of the LCF7, with two different diameters of fluorine-doped silica rods, as shown in Fig. 3. This is designed to increase the HOM leakage loss [14], while keeping the FM one low enough. Figure 3(a) shows the cross-section of an LCF7 formed by twelve fluorine-doped silica rods with diameters d_1 and d_2 ($d_1 > d_2$), alternately arranged. This design is denoted through the paper as LCF7-1, and features a six-fold symmetry. Figures 3(b) and 3(c) show the cross-section of LCF7 designs with the same diameters d_1 and d_2 ($d_1 > d_2$), but having two-fold symmetry (LCF7-2 and LCF7-3, respectively). In Figs. 4(a), 4(b), and 4(c), we show the FM effective area contour plots at 1064 nm as a function of the design parameters Λ and d_2/Λ for the LCF7-1, LCF7-2, and LCF7-3, respectively. Here, the value of the normalized fluorine-doped rod diameter d_1/Λ is fixed at $d_1/\Lambda = 0.95$ to obtain low bending loss. Notice that, due to the two-fold symmetry structure, the effective areas and effective indices of the FMs in LCF7-2 and LCF7-3 have a theoretical polarization dependence. However, it is negligibly small at 1064 nm, since the two fibers have large core size, so that their geometrically induced birefringence is less than 10^{-7}. As before, the solid black curve corresponds to a HOM CL of 1 dB/m and the dashed black curve to a FM CL of 0.1 dB/m, at 1064 nm wavelength. The variation trend of the effective area is almost the same in each of LCF7-1, LCF7-2, and LCF7-3. In addition, we can see from Fig. 4(a) that LCF7-1 has no possibility to fulfill both $CL_{\mathrm{fund}} < 0.1$ dB/m and $CL_{\mathrm{2nd}} > 1$ dB/m, simultaneously. On the other hand, in LCF7-2 and LCF7-3, the
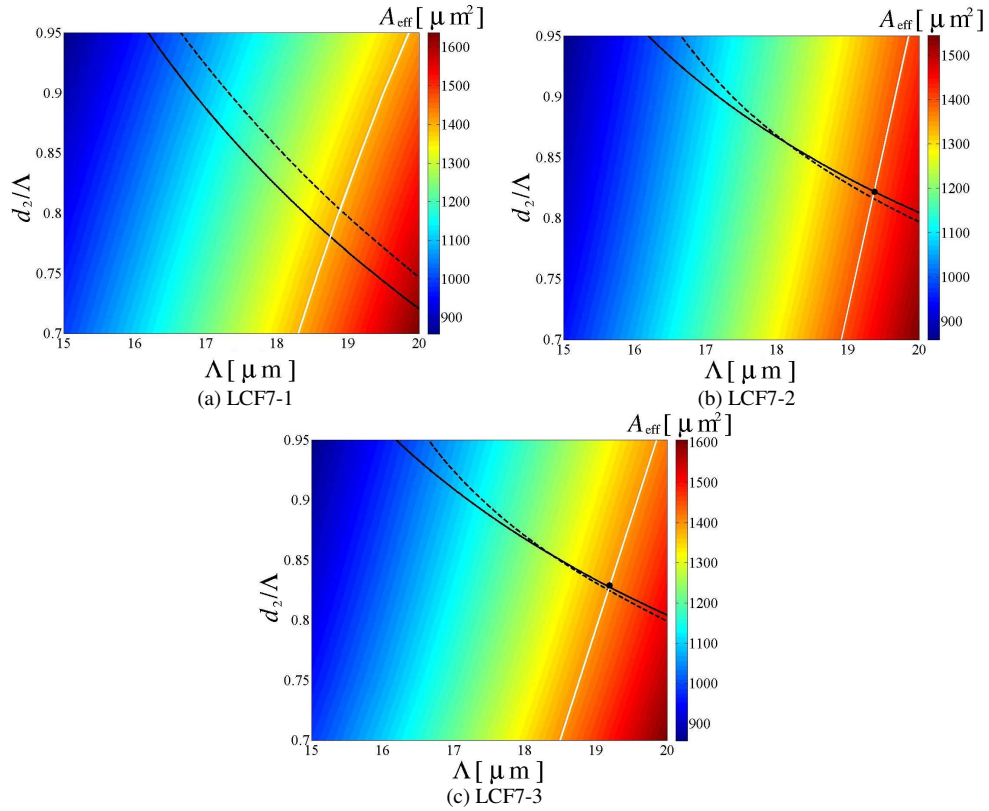
Fig. 4. Effective area of FM at 1064 nm as a function of Λ and d_2/Λ for (a) LCF7-1 (b) LCF7-2, and (c) LCF7-3, for constant $d_1/\Lambda = 0.95$.
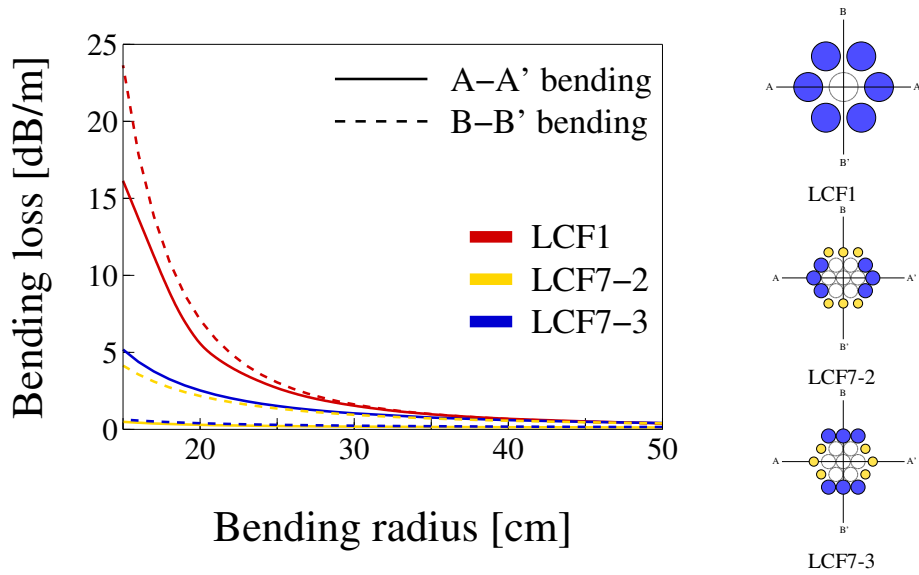
Fig. 5. Bending loss in dB/m as a function of the bending radius in cm at 1064 nm. The red curve corresponds to the LCF1 with $\Lambda = 42.3$ μm, $d/\Lambda = 0.81$, while the yellow and blue curves correspond to the LCF7-2 with $\Lambda = 19.4$ μm, $d_1/\Lambda = 0.95$, $d_2/\Lambda = 0.82$ and LCF7-3 with $\Lambda = 19.2$ μm, $d_1/\Lambda = 0.95$, $d_2/\Lambda = 0.82$, respectively.
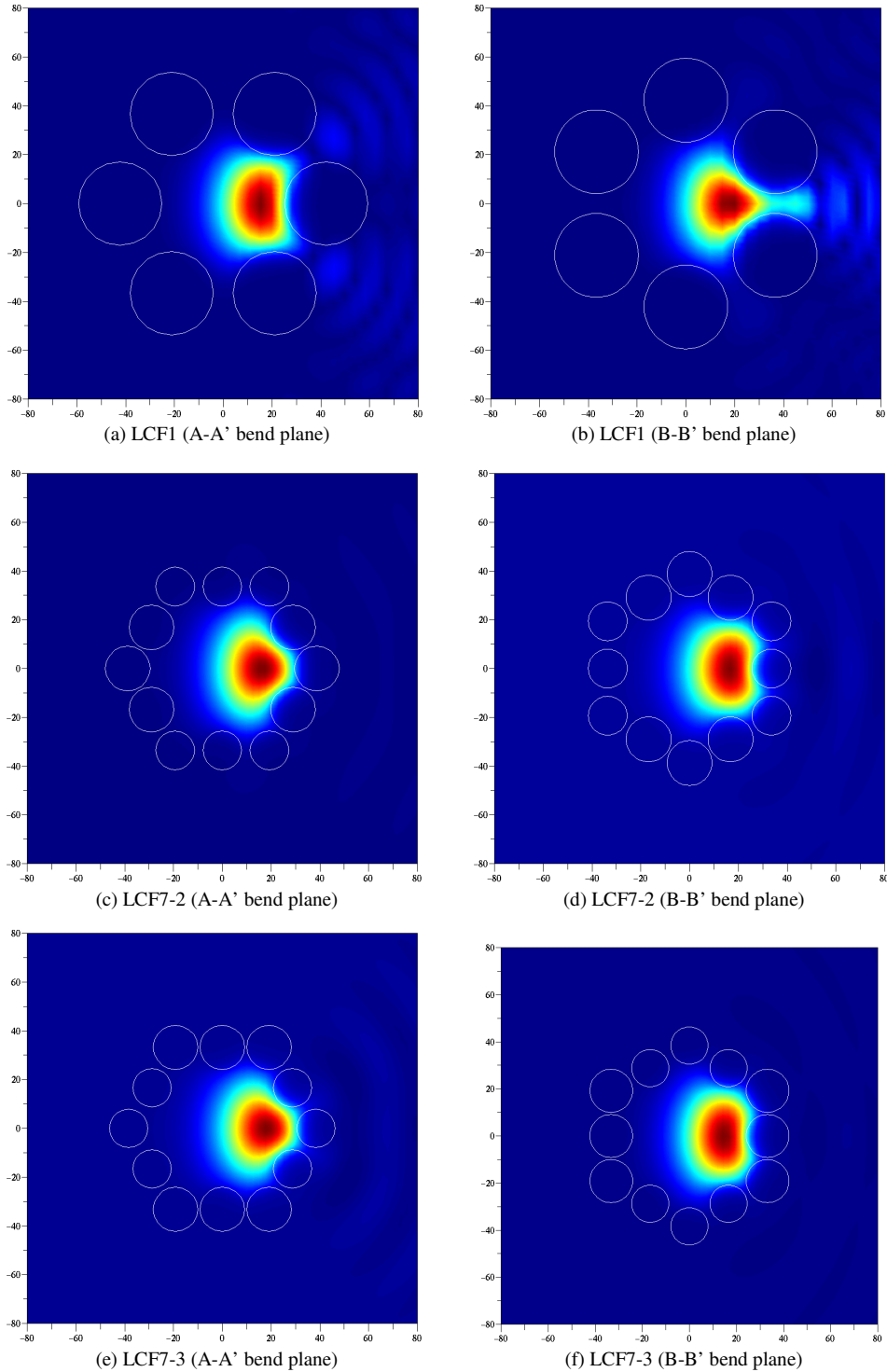
Fig. 6. Simulated optical field distributions of FM at 1064 nm in the bent LCF1 (Λ = 42.3 μm, d/Λ = 0.81), LCF7-2 (Λ = 19.4 μm, d_1/Λ = 0.95, d_2/Λ = 0.82), and LCF7-3 (Λ = 19.2 μm, d_1/Λ = 0.95, d_2/Λ = 0.82) fibers, with a 15-cm bending radius for both A-A' and B-B' bend planes. For the B-B' bend plane simulation, the fiber is rotated by 90 degrees.

solid black curve intersects the dashed one, as shown in Figs. 4(b) and 4(c). This indicates that LCF7-2 and LCF7-3 can achieve effectively single-mode operation. Specifically, we can set the structural parameters of LCF7-2 and LCF7-3 to simultaneously realize this condition and A_{eff} = 1400 μm^2, obtaining Λ = 19.4 μm, d_1/Λ = 0.95, and d_2/Λ = 0.82 for the LCF7-2, and Λ = 19.2 μm, d_1/Λ = 0.95, and d_2/Λ = 0.82 for the LCF7-3, corresponding to the black circles in Figs. 4(b) and 4(c), respectively.

Next, we show in Fig. 5 the numerically calculated FM bending loss at 1064 nm as a function of bending radius in LCF1 (Λ = 42.3 μm, d/Λ = 0.81), LCF7-2 (Λ = 19.4 μm, d_1/Λ = 0.95, d_2/Λ = 0.82), and LCF7-3 (Λ = 19.2 μm, d_1/Λ = 0.95, d_2/Λ = 0.82). We employed the V-FEM solver in a local cylindrical coordinate system [13] for efficient and accurate analysis of the bending loss in curved LCFs. The solid curve corresponds to the bending plane indicated by A-A' and the dashed curve to the B-B' one, respectively. Since these three all-glass LCFs all have the same effective area and the same HOM CL, we could expect that they would show similar macro-bending loss characteristics. Surprisingly, the LCF7-2 and LCF7-3 proposed here show totally different bending losses and can achieve much lower values, compared with LCF1. Moreover, LCF7-2 has a slightly lower bending loss as compared with LCF7-3, due to the fluorine-doped silica rod orientation. The LCF7-2 bent parallel to the A-A' plane has the lowest bending loss of less than 0.5 dB/m for a 15-cm bending radius.

Finally, in Fig. 6 we plot the simulated optical field distributions in the curved LCF1, LCF7-2, and LCF7-3 at the operating wavelength of 1064 nm and the bending radius of 15 cm for both A-A' and B-B' bending planes. As we can see, the optical field spreads out into the outer cladding of LCF1, whereas on the other hand, the fields are still confined into the solid core of LCF7-2 and LCF7-3. It is important to underline that the rod-to-rod gap width, defined as the difference between the pitch and the rod diameter, in LCF7-2 or LCF7-3 is much smaller than that in LCF1, therefore, a better FM confinement in the LCF7-2 and LCF7-3 is expected. Notice that the decrement of the rod-to-rod gap width results in a decrement of the loss ratio $CL_{2nd}/CL_{\text{fund}}$, however, sufficient differential mode loss of $CL_{2nd}/CL_{\text{fund}} > 10$ with core diameter of larger than 50 μm can be achieved by LCF7-2 and LCF7-3 configurations.

3. Conclusions

We have proposed and numerically investigated a novel type of all-glass LCFs having an effective area of 1400 μm^2 with effectively single-mode behavior. We found that the LCFs having a seven-cell solid core and two different fluorine-doped silica rod diameters arranged in accordance with a two-fold symmetry (as opposed to the more natural six-fold one) can achieve a large core diameter of around 50 μm, effectively single-mode operation, and low bending loss, below 0.5 dB/m at 1064 nm for a bending radius of 15 cm.

Acknowledgments